World Applied Sciences Journal 29 (10): 1301-1309, 2014
ISSN 1818-4952

DOI: 10.5829/idosi.wasj.2014.29.10.1581

Comparison Between 2D and 3D Simulations of a Tray Dryer System Using CFD Software

[1,2]S. Misha,[1]S. Mat, [1]M.H. Ruslan,[1]K. Sopian and [1]E. Salleh

[1]Solar Energy Research Institute, Universiti Kebangsaan Malaysia,
43600 Bangi Selangor, Malaysia
[2]Faculty of Mechanical Engineering, Universiti Teknikal Malaysia Melaka,
Hang Tuah Jaya, 76100 Durian Tunggal, Melaka, Malaysia

Submitted: Dec 18, 2013; **Accepted:** Jan 25, 2014; **Published:** Jan 28, 2014

Abstract: The tray dryer is the most extensively used drying system because of its simple and economic design. The drawback of this dryer is the non-uniformity in the final moisture content of the product. This research aims to predict the temperature and velocity profile in the drying chamber using computational fluid dynamics simulations. Two 3D designs of drying chambers (cases 1 and 2) were studied. Both designs have the same dimensions, except for the geometry of the inlet and outlet boundary conditions. The simulation was performed in 3D, but the analysis was carried out in a 2D plane. Another 2D simulation (case 3) was carried out to compare the results with those of the 3D simulation. The design in case 2 can be represented in a 2D simulation, whereas the design in case 1 must be represented in a 3D simulation. The 3D simulation can be simplified into a 2D simulation if the geometry and boundary conditions in the 3D simulation are the same as those in the 2D simulation at any position of the plane parallel to the 2D drawing. The 2D simulation is simple and saves time in terms of design, meshing and iteration processes for achieving convergent solutions.

Key words: Drying simulation · Tray dryer · Uniform drying

INTRODUCTION

The tray dryer is widely used in a variety of applications because of its simple design and capacity to dry a large number of products. However, the biggest drawback of the tray dryer is uneven drying caused by the poor airflow distribution in the drying chamber. Several designs and methods can be implemented to improve the performance of tray dryers; the improvements can enhance the quality of the dried product and ensure uniform drying, as reported by Misha *et al*. [1].

The measurement of temperature, humidity and velocity in the drying chamber is expensive, difficult and time consuming because many sensors must be installed in several positions, especially in a large-scale dryer. Computational fluid dynamics (CFD) simulation is widely used because equations for the conservation of mass, momentum and energy can be solved using numerical methods to predict the temperature, velocity and pressure profiles in the drying chamber. CFD is considered an integral part of engineering design and analysis because it can predict the performance of new designs.

Mathioulakis *et al*. [2] designed and constructed an industrial batch-type tray dryer for drying fruits. CFD was used to simulate the air velocity and the pressure profiles in the drying chamber. The result shows that a variation in final moisture content occurs in several trays. A comparison between the CFD simulation result and experimental data shows a strong correlation between drying rate and air velocity. Dionissios and Adrian-Gabriel Ghious [3] studied the numerical simulation inside a drying chamber. A set of measurements was obtained experimentally above one single tray to validate the model. The

Corresponding Author: S. Misha, Faculty of Mechanical Engineering, Universiti Teknikal Malaysia Melaka, Hang Tuah Jaya, 76100 Durian Tunggal, Melaka, Malaysia. Tel.: +60 6 2346712, Fax: +6 06 2346884.

validation between the measured data and the simulation results by CFD shows that the standard k–e model is the most adequate turbulence model.

Mirade [4] used a two-dimensional CFD model with time-dependent boundary conditions to investigate the homogeneity of the distribution of the air velocity in an industrial meat dryer for several low and high levels of the ventilation cycle. All airflow simulations are consistent with the heterogeneity of drying usually observed in practice. The product is represented by a solid rectangular object. Chr. Lamnatou *et al*. [5] constructed and investigated a numerical model of heat and mass transfer during convective drying of a porous body using the finite volume method. The aspect ratio of the drying plate and the flow separation affect the flow field and heat/mass transfer coefficients. The increase in the contact surfaces between the air and porous body also contributes to the improvement of drying behavior. Some products can be treated as solid (non-porous) material. However, most products are represented by porous media. Overall velocities in the drying chamber are lower when porous products are used than when solid products are utilized because some of the hot air stream pass through porous products [6].

Amanlou and Zomorodian [7] studied a new cabinet dryer with a side-mounted plenum chamber for fruit drying. Experimental work and simulations by CFD were carried out to achieve uniform drying. The developed dryer produces uniform airflow and temperature distribution in the drying chamber. Jacek Smolka *et al*. [8] studied a numerical model of a drying oven using CFD simulation. Several new configurations were simulated to improve the uniformity of temperature in the drying chamber. A new shape and an additional baffle were found to be the most effective improvements. In both cases, the simulation results show very good agreement with the experimental data.

The present study aims to predict the drying uniformity of the final moisture content of the product by studying the temperature and velocity profile in the drying chamber using CFD simulation. The moisture content is determined by using load cell to get the difference between final and initial mass of the product. Bakhshipour *et al*. [9] used a machine vision system integrated with the neural networks to predict the moisture content of raisin. CFD simulation in 2D and 3D is carried out. The comparison of the simulation result will show which 3D design can be represented by 2D simulation. CFD has been extensively used in the food industry to investigate the airflow pattern in drying chambers [10], [11]. Uniform airflow distribution in a drying chamber is very important because it strongly influences dryer efficiency and the homogeneity of the products being dried [4]. The use of a desiccant material in drying applications has several advantages, including the improvement in the uniformity of dried products [12].

METHODS AND SIMULATION

Design of the Drying Chamber: The basic design of the drying chamber is shown in Figure 1. The wall of the dryer system was constructed using 6 cm thick hollow polycarbonate with a hollow space in the middle measuring 4 cm deep. The drying chamber dimension is

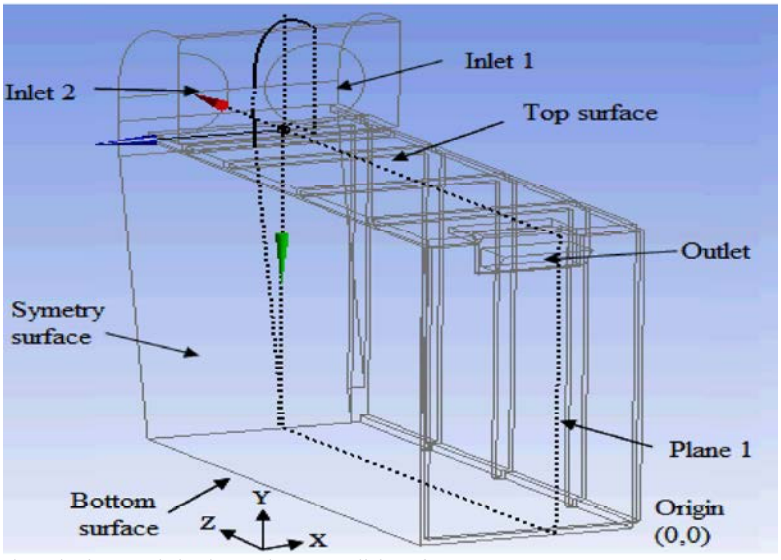

Fig. 1: 3D drying chamber design and the boundary condition for case 1.

approximately 2 m x 3 m x 1.7 m (width, length and height, respectively). The dryer system consists of seven levels of tray systems, each of which has three separate trays. The thickness of the products in each tray is 6 cm. The velocity and temperature distribution were analyzed to predict the drying uniformity in the drying chamber.

Basic Governing Equations for Designing the Tray Dryer: The mass, momentum and energy conservation result in the continuity, Navier–Stokes and energy equations, respectively [13]. The turbulent model is used in this CFD simulation. The turbulent kinetic energy, k and its rate of dissipation, ε, are calculated from the following transport equations [14]:

$$\frac{\partial}{\partial t}(\rho k)+\frac{\partial}{\partial x_i}(\rho k u_i)=\frac{\partial}{\partial x_j}\left[\left(\mu+\frac{\mu_t}{\sigma_k}\right)\frac{\partial k}{\partial x_j}\right]G_k+G_b-\rho\varepsilon-Y_M+S_k \tag{1}$$

$$\frac{\partial}{\partial t}(\rho \varepsilon)+\frac{\partial}{\partial x_i}(\rho \varepsilon u_i)=\frac{\partial}{\partial x_j}\left[\left(\mu+\frac{\mu_t}{\sigma_\varepsilon}\right)\frac{\partial \varepsilon}{\partial x_j}\right]C_{1\otimes\otimes}\frac{\varepsilon}{k}(G_k-C_{3\varepsilon}G_b)-C_{2\varepsilon}\rho\frac{\varepsilon^2}{k}+S_\varepsilon \tag{2}$$

Convective heat and mass transfer modeling in the k–ε models is given by the following equation:

$$\frac{\partial}{\partial t}(\rho E)+\frac{\partial}{\partial x_i}[u_i(\rho E+p)]=\frac{\partial}{\partial x_i}\left[\left(k+\frac{C_p\mu_t}{\Pr_t}\right)\frac{\partial T}{\partial x_i}+u_i(\tau_{ij})eff\right]+S_h \tag{3}$$

Product trays are assumed to be porous media for airflow. Porous media are modeled by adding a momentum source term to the standard fluid flow equations. The source term is composed of two parts: a viscous loss term and an inertial loss term.

$$S_i=-\left(\sum_{j=1}^{3}D_{ij}\mu v_j\sum_{j=1}^{3}C_{ij}\frac{1}{2}\rho v_{mag}v_i\right) \tag{4}$$

Simulation Details: The numerical finite volume method, as used in Fluent 14.0, has been used to solve equations and to build a numerical model based on an unstructured 3D mesh by tetrahedral cells. The pattern of air stream in the drying chamber is important and because variable condition was absent in the current study, the simulation was carried out in a steady state condition. In case 1, plane 1 was selected (Figure 1) to study and analyze the velocity and temperature in the drying chamber. Plane 1 is located in the center of the fans. Three simulations were carried out to predict the temperature and velocity distributions in the drying chamber using 2D and 3D CFD simulations. The simulations in cases 1 and 2 were performed in 3D but with different inlet and outlet conditions. In case 2, the inlet area is rectangular, whereas the outlet area is found along the X-axis (Figure 2). The simulation in case 3 was performed in 2D (Figure 3). The position of the trays for all cases is shown in Figure 4 (case 1). The set up of the boundary

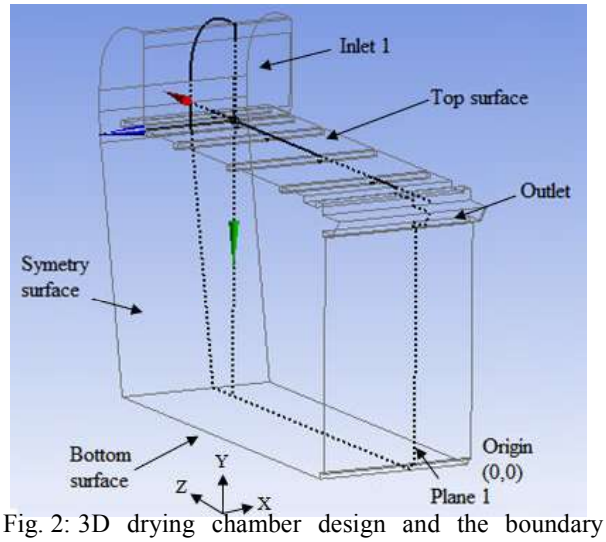

Fig. 2: 3D drying chamber design and the boundary condition for case 2.

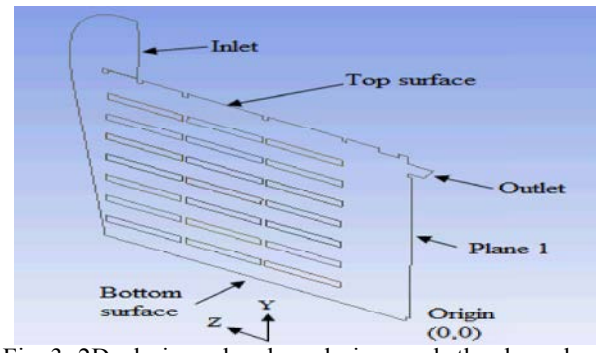

Fig. 3: 2D drying chamber design and the boundary condition for case 3.

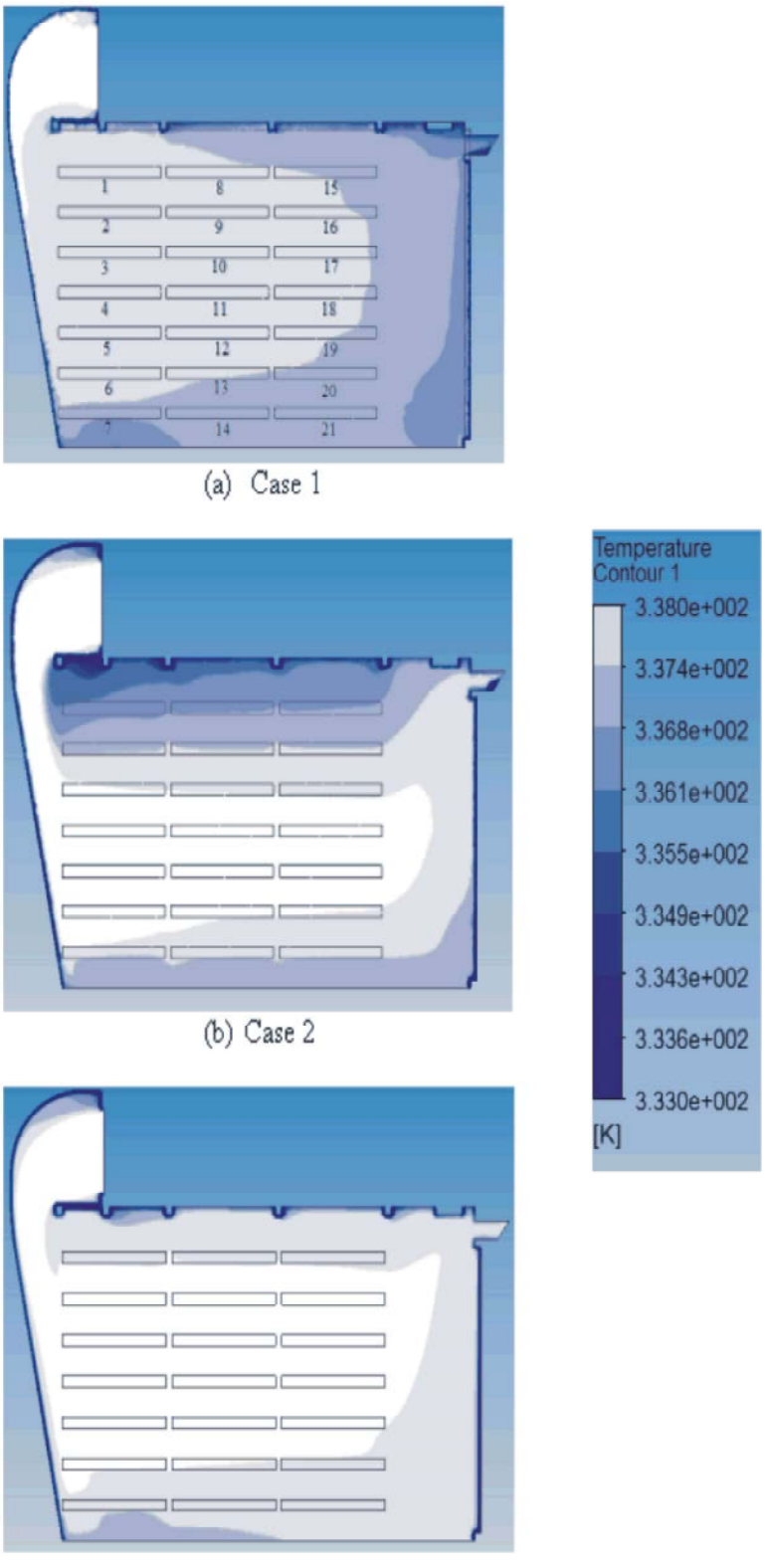

(a) Case 1

(b) Case 2

(c) Case 3

Fig. 4: Temperature distribution profiles using CFD simulations at plane 1.

Table 1: Boundary condition for each case

Boundary Condition	3D		2D
	Case 1	Case 2	Case 3
Inlet 1	Air mass flow rate 0.5843 kg/s (velocity of 3 m/s normal to air inlet) and air temperature of 65°C.	Air mass flow rate 1.6372 kg/s (velocity of 3 m/s normal to air inlet) and air temperature of 65°C.	Air velocity 3 m/s and temperature 65°C.
Inlet 2	Air mass flow rate 0.2922 kg/s (half of the inlet 1 but give same velocity, 3 m/s) and air temperature of 65°C.	Nil	Nil
Outlet	Assuming gauge pressure = 0		
Porous media	The trays were assumed as porous media with 10% porosity.		
Wall	Heat transfer coefficient of the chamber wall and environmental conditions were defined. The environment temperature is assumed at 33°C and temperature at the top roof is 55°C (contact to the heat source from radiation). The bottom surface is assumed as no heat loss. Only half of the drying chamber was analysed since the shape is symmetry by defining the symmetry surface to the middle boundary.		The environment temperature is assumed at 33°C and temperature at the top roof is 55°C. The bottom surface is assumed as no heat loss.

conditions for each case is defined in Table 1. The dryer is designed for any agricultural product; however, in this simulation, the properties of chipped kenaf core are applied to the product as an example. The size or dimension of the chipped kenaf core was reported by Misha *et al*. [15].

RESULT AND DISCUSSION

In the 3D simulations (cases 1 and 2), plane 1 was selected to study the airflow distribution because its geometry is identical to that in the 2D simulation (case 3). In case 2, cutting at any point on the YZ plane results in the same geometry as that in the 2D simulation. By contrast, cutting at any other point on the YZ plane in case 1 results in a different geometry; that is, the inlet dimension is small and an inlet or outlet boundary is absent in some planes. This result is attributed to the inlet boundary being circular and to the outlet boundary being absent along the X-axis. As the geometry in plane 1 (cases 1 and 2) and that in the 2D simulation are exactly the same, comparisons can easily be done for each case. The numbers of trays from 1 to 21 are indicated in Figure 4 (case 1).

The temperature distribution in the drying chamber is shown in Figure 4. The hot air temperature at the inlet is 65°C. In case 1, the temperature of trays 7, 13, 14, 15, 20 and 21 ranges from 63.8°C to 64.4°C. The temperature of the rest of the trays is higher than 64.4°C, with the highest temperature being 65°C. In case 2, the temperature of the trays at the first and second levels from the top is between 63.1°C and 64.4°C. In case 3, the temperature of all the trays ranges from 64.4°C to 65°C. The temperature difference among the trays in all cases is considered small. Therefore, all designs can be assumed to have successfully achieved uniform air temperature in the drying chamber.

In drying applications, the temperature, velocity and humidity of the drying air significantly affect the drying process. In this simulation study, only the temperature and velocity of the drying air can be analyzed because the equation utilized in the analysis does not involve humidity. Humidity analysis will be done in future experimental work. The air velocity above the trays is very important in removing moisture from the products. The air velocity profile at 2.5 cm above each tray of plane 1 is shown in Figure 5. Generally, the average air velocities in trays 1 to 7 are higher than those in the other trays because they are positioned very close to the inlet. In case 1, the air velocities range from 0.26 m/s to 1.10 m/s, with an average velocity of approximately 0.35 m/s. In cases 2 and 3, the air velocities range from 0 m/s to 3.85 m/s, with an average velocity of approximately 1.10 m/s. The velocity values for each tray in cases 2 and 3 are not identical, but they follow the same pattern. The average velocities for each line (cases 2 and 3) are shown in Table 2. The maximum difference is 0.27 m/s, the minimum difference is 0.01 m/s and the average difference is 0.18 m/s.

In all cases, the air velocity decreases as the drying air passes over the trays, except for the tray at the highest level. The positions of trays 1, 8 and 15 are closer to the air inlet and outlet compared with those of the other trays. The air velocity at the inlet for all cases is 3 m/s; however, the mass flow rate in the 3D simulations (cases 1 and 2) is different. The mass flow rate of case 2 is almost twice that of case 1. Thus, the air velocity in case 1 is much lower than that in case 2. The air velocity in the trays at the top

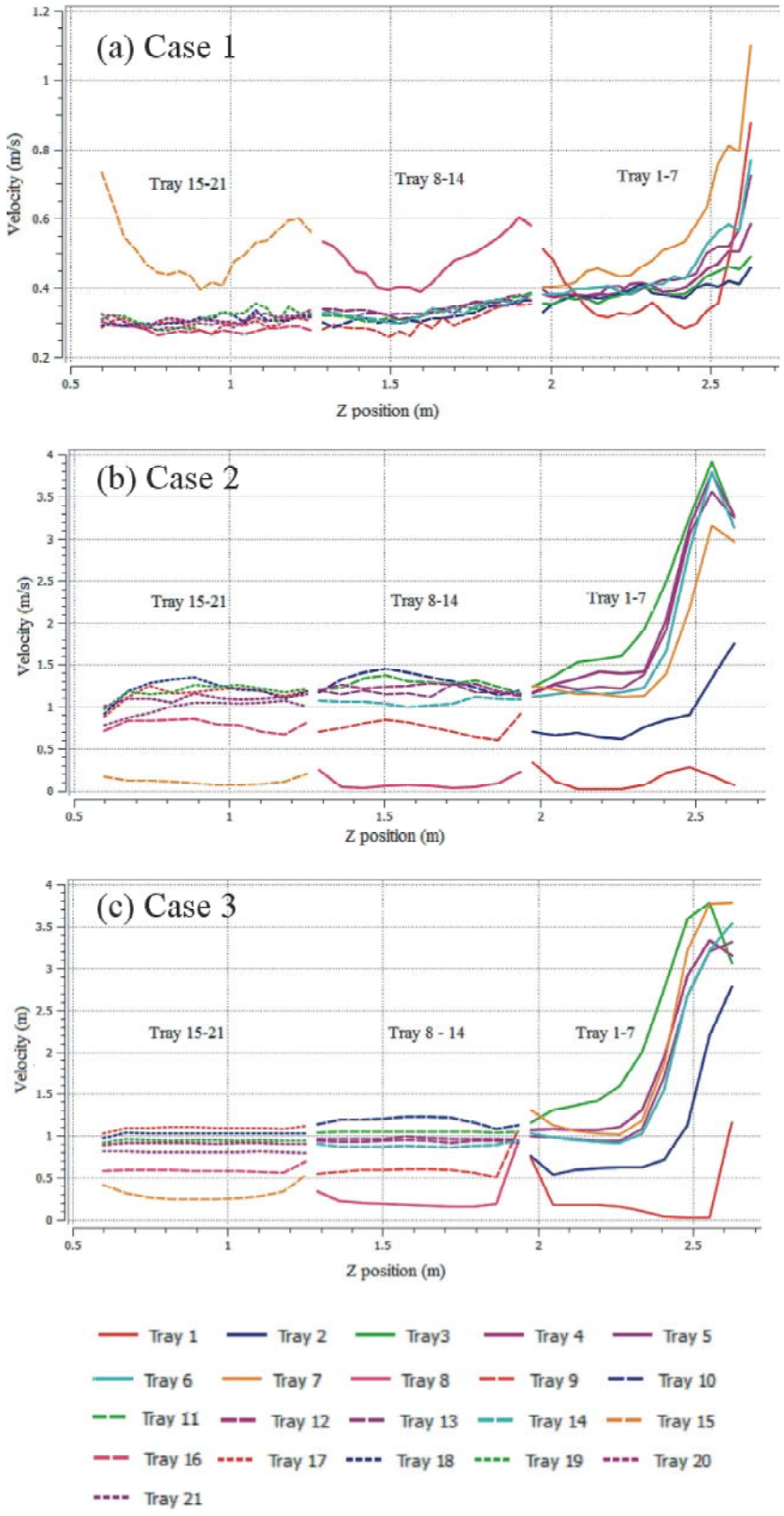

Fig. 5: Result of air velocity against tray positions (along Z axis) at plane 1.

Table 2: Average velocity above the tray at plane 1

Tray number	Average velocity above the tray (m/s) Case 2	Case 3	Difference (m/s)
1	0.13	0.28	0.15
2	0.89	1.06	0.16
3	2.21	2.20	0.01
4	2.02	1.80	0.22
5	1.92	1.68	0.25
6	1.84	1.68	0.17
7	1.67	1.93	0.27
8	0.09	0.27	0.18
9	0.75	0.62	0.13
10	1.30	1.18	0.12
11	1.27	1.04	0.23
12	1.23	0.96	0.27
13	1.17	0.93	0.24
14	1.05	0.88	0.17
15	0.11	0.31	0.20
16	0.78	0.59	0.19
17	1.15	1.09	0.06
18	1.20	1.02	0.18
19	1.18	0.94	0.24
20	1.09	0.91	0.19
21	0.98	0.81	0.18
	Maximum average velocity	0.27	
	Minimum average velocity	0.01	
	Average of difference between case 2 and 3	0.18	

level (trays 1, 8 and 15) is high in case 1 and low in cases 2 and 3. In case 1, the air velocity is low (less than 1.9 m/s) after collision with the curved wall; the air is distributed to all levels, including the top tray. In cases 2 and 3, the air velocity is high (greater than 2.6 m/s) after collision with the curved wall; the air is distributed mostly to the trays at the lower levels. Therefore, the trays at the first and second levels have lower velocity than the other trays in cases 2 and 3. The details of the velocity distribution profile for each case are shown in Figure 6.

The result of case 1 differs from the results of cases 2 and 3. Although the air velocity at the inlet of the selected plane is the same (3 m/s), the inlet geometry in case 1 is not the same when the YZ plane is cut at different points. In case 2, the same geometry, including that of the inlet, is achieved when the YZ plane is cut at any point. Therefore, the 3D simulation in case 2 can be represented by a 2D simulation as in case 3. Simulation in 3D is very complex and time consuming in terms of design, meshing and iteration processes for achieving convergent solutions. The time required to process the results in cases 1 and 2 is approximately two hours, whereas that in case 3, which used 2D simulation, is only three minutes. If possible, 2D simulation is thus

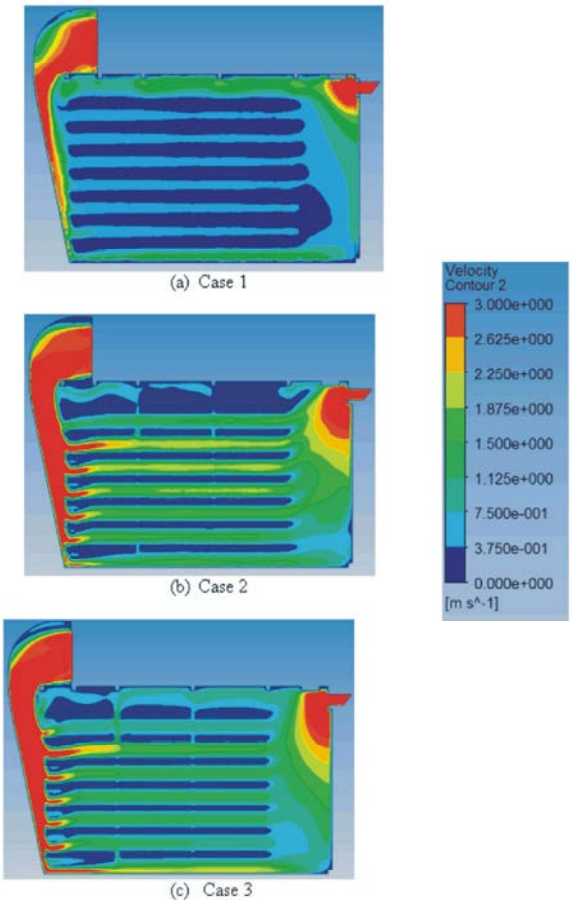

Fig. 6: Velocity distribution profiles using CFD simulations at plane 1.

preferable. However, not all 3D problems can be simplified into 2D simulations. In this study, presenting the design of the drying chamber in 2D, as in case 1, is impossible because the inlet geometry is not the same when the YZ plane is cut at any point.

Basically, a problem can be represented in 2D if the shape or geometry and boundary condition of the 3D problem are the same with the 2D drawing at any point of the plane parallel to the 2D drawing. Otherwise, the results of the 2D simulation may not be consistent with the results of the 3D simulation. The result of the 3D simulation in case 2 is different from the result of the 2D simulation in case 3 because on the one hand, the actual airflow streamline in 3D moves not only across plane 1 but also over other positions. On the other hand, the airflow streamline in 2D only moves across one plane; therefore, the pattern is very linear.

Mesh generation in 3D is complicated and requires some skill to obtain satisfactory meshing. In this study, mesh adaption was performed to ensure mesh-

independent solution and to obtain accurate results. In future experimental work, several positions in the drying chamber should be installed with temperature, velocity and humidity sensors to validate the simulation data.

CONCLUSION

Good airflow distribution in a drying chamber can improve drying uniformity. CFD simulation is very useful in predicting the air velocity and temperature profiles in a drying chamber. Simulation in 3D provides superior results because it represents the actual problem, but it is expensive and time consuming. Therefore, 2D simulation may be carried out in some cases to solve the simulation work. Simulation in 3D can be simplified into simulation in 2D if the shape or geometry and boundary condition in 3D are the same as that in 2D at any point of the plane parallel to the 2D drawing. In this study, the 3D drying chamber in case 2 could be presented in 2D. The results are not exactly the same, but the average velocity and the velocity and temperature ranges are consistent. In case 1, the simulation was carried out in 3D. Simulation in 3D is complex and time consuming in terms of design, meshing and iteration processes for achieving convergent solutions. Additional baffles may be used to distribute the airflow evenly to each tray level. Uniform drying and increase in drying rate will improve the quality of the dried product. In the future, the experimental work will be carried out for agricultural drying to validate the simulation data.

ACKNOWLEDGEMENTS

The authors would like to thank the Solar Energy Research Institute, Universiti Kebangsaan Malaysia and Universiti Teknikal Malaysia Melaka for sponsoring this work.

Nomenclature:

C, D	Prescribed matrices
C_0, C_1	empirical coefficients
C_{ij}	prescribed matrices
Dij	mass diffusion coefficient
ρ	density of fluid
k	turbulent kinetic energy
ε	rate of dissipation
μ	dynamic viscosity
μ_t	turbulent viscosity
G_k	generation of turbulent kinetic energy due to the mean velocity gradients
G_b	generation of turbulent kinetic energy due to buoyancy
Y_M	contribution of the fluctuating dilatation in compressible turbulence to the overall dissipation rate S_i
C_1, C_2, C_3	constants used in turbulent model
σ_k	turbulent Prandtl numbers for k
σ_ε	turbulent Prandtl numbers for ε
E	total energy
v_i	velocity vector
v_{mag}	velocity magnitude
$(\tau_{ij})_{eff}$	deviatoric stress tensor
p	pressure
Pr_t	Prandtl number
T	temperature
c_p	specific heat capacity at constant pressure
u	velocity magnitude in x direction
t	time
S_k, S_ε,S_h	user-defined source terms source term for ith momentum dissipation rate equation

REFERENCES

1. Misha, S., S. Mat, M.H. Ruslan, K. Sopian and E. Salleh, 2013. Review on the application of a tray dryer system for agricultural products. World Applied Sciences Journal, 22(3): 424-433.
2. Mathioulakis, E., V.T. Karathanos and V.G. Belessiotis, 1998. Simulation of air movement in a dryer by computational fluid dynamics: Application for the drying of fruits.Journal of Food Engineering, 36(2): 183-200.
3. Margaris, D.P. and A.G. Ghiaus, 2006. Dried product quality improvement by air flow manipulation in tray dryers.Journal of Food Engineering, 75(4): 542-550.
4. Mirade, P.S., 2003. Prediction of the air velocity field in modern meat dryers using unsteady computational fluid dynamics (CFD) models.Journal of Food Engineering, 60(1): 41-48.
5. Lamnatou, C., E. Papanicolaou, V. Belessiotis and N. Kyriakis, 2010. Finite-volume modelling of heat and mass transfer during convective drying of porous bodies - Non-conjugate and conjugate formulations involving the aerodynamic effects. Renewable Energy, 35(7): 1391-1402.
6. Misha, S., S. Mat, M.H. Ruslan, K. Sopian and E. Salleh, 2013. Comparison of CFD simulation on tray dryer system between porous and solid product. In the Proceedings of the 7th WSEAS International Conference on Renewable Energy Sources (RES' 13), pp: 59-64.

7. Amanlou, Y. and A. Zomorodian, 2010. Applying CFD for designing a new fruit cabinet dryer.Journal of Food Engineering, 101(1): 8-15.
8. Smolka, J., A.J. Nowak and D. Rybarz, 2010. Improved 3-D temperature uniformity in a laboratory drying oven based on experimentally validated CFD computations. Journal of Food Engineering, 97(3): 373-383.
9. Bakhshipour, A., A. Jafari and A. Zomorodian, 2012. Vision based features in moisture content measurement during raisin production. World Applied Sciences Journal, 17(7): 860-869.
10. Verboven, P., N. Scheerlinck, J. De Baerdemaeker and B.M. Nicola, 2000. Computational fuid dynamics modelling and validation of the temperature distribution in a forced convection oven.Journal of Food Engineering, 43: 61-73.
11. Scott, G. and P. Richardson, 1997. The application of computational fluid dynamics in the food industry. Trends in Food Science & Technology, 8(4): 119-124.
12. Misha, S., S. Mat, M. Ruslan and K. Sopian, 2012. Review of solid/liquid desiccant in the drying applications and its regeneration methods. Renewable and Sustainable Energy Reviews, 16(7): 4686-4707.
13. Norton, T. and D.W. Sun, 2006. Computational fluid dynamics (CFD) - an effective and efficient design and analysis tool for the food industry: A review.Trends in Food Science & Technology, 17(11): 600-620.
14. Yongson, O., I.A. Badruddin, Z.A. Zainal and P.A. Aswatha Narayana, 2007. Airflow analysis in an air conditioning room. Building Environment, 42(3): 1531-1537.
15. Misha, S., S. Mat, M.H. Ruslan, K. Sopian and E. Salleh, 2013. The effect of drying air temperature and humidity on the drying kinetic of kenaf core.Applied Mechanics and Materials, 315: 710-714.